



Controlling Polarization in Quantum-dot Semiconductor Optical Amplifiers

Yasuoka, Nami ; Ebe, Hiroji ; Kawaguchi, Kenichi ; Ekawa, Mitsuru ;
Kita, Takashi ; Wada, Osamu ; Sugawara, Mitsuru ; Saito, toshio ;...

(Citation)

Memoirs of the Graduate School of Engineering Kobe University, 1:1-8

(Issue Date)

2009

(Resource Type)

departmental bulletin paper

(Version)

Version of Record

(URL)

<https://hdl.handle.net/20.500.14094/81002730>



Controlling Polarization in Quantum-dot Semiconductor Optical Amplifiers

Nami YASUOKA¹, Hiroji EBE², Kenichi KAWAGUCHI³,
Mitsuru EKAWA⁴, Takashi KITA⁵, Osamu WADA⁶,
Mitsuru SUGAWARA⁷, Toshio SAITO⁸, and Yasuhiro ARAKAWA⁹

¹ *Fujitsu Limited and Optoelectronic Industry and Technology Development Association*

² *Institute for Nano Quantum Information Electronics (INQIE), The University of Tokyo*

³ *Fujitsu Limited and Optoelectronic Industry and Technology Development Association*

⁴ *Fujitsu Laboratories Limited*

⁵ *Department of Electrical and Electronics Engineering, Faculty of Engineering, Kobe University*

⁶ *Department of Electrical and Electronics Engineering, Faculty of Engineering, Kobe University*

⁷ *Fujitsu Laboratories Limited and QD Laser Incorporated*

⁸ *Institute for Nano Quantum Information Electronics (INQIE), The University of Tokyo*

⁹ *Institute for Nano Quantum Information Electronics (INQIE), Institute of Industrial Science (IIS), Research Center for Advanced Science and Technology (RCAT), The University of Tokyo*

(Received November 13, 2009; Accepted January 12, 2010; Online published January 18, 2010)

Keywords: semiconductor optical amplifier, quantum dots, polarization

The possibility of applying a polarization-insensitive quantum-dot (QD) semiconductor optical amplifier (QD-SOA) to future optical communication systems is demonstrated. It was found that the optical-polarization property of a QD depends on both its aspect ratio and strain. To control these two parameters, a columnar QD (CQD), which has a high aspect ratio and is surrounded by side-barriers, was optimized. These optimized CQDs demonstrated polarization-insensitive characteristics in the 1.5- μm wavelength band. Moreover, they have a gain of 10.0 dB with low (i.e., ± 0.9 dB) polarization dependence.

Introduction

Quantum-dot semiconductor optical amplifiers (QD-SOAs) are attractive devices for next-generation optical-network systems owing to their distinctive features such as broadband gain, high-speed response, and high-saturation output power^{1)–13)}. In the case of many optical communication systems, polarization-insensitive optical properties of QD-SOAs are required. The polarization of an optical signal in standard fiber is random, and the randomly polarized signal limits the applicability of optical communication systems. However, QDs grown in the conventional Stranski-Krastanow (SK) mode exhibit much more transverse-electric (TE)-mode gain than transverse-magnetic (TM)-mode gain. A few different approaches^{14)–16)} have been proposed to solve this problem. One method is to control polarization anisotropy in the gain material itself. However, to develop polarization-insensitive SOA chips, this method must be investigated in more detail. This method has the advantages of reducing the size and cost of the SOA module. For example, standard multiple-quantum-well (MQW) materials in SOAs also exhibit larger TE-mode gain than TM-mode gain. Polarization-insensitive gain has been obtained by using tensile-strained barriers in MQWs as an active layer^{17), 18)}. For QDs, the TE-dominant polarization properties are due to SK-mode-grown QD structures with half-oval shapes and biaxial compressive strains. Under these conditions, electronic

states are strongly quantized in the vertical direction, and valence bands are split into heavy-hole (HH) and light-hole (LH) bands, where the HH valence band edge (E_{HH}) is higher than the LH one (E_{LH}). Since the TM transition between the conduction band and the HH band is prohibited by the selection rule, the optical transition in TE mode is predominant^{19)–20)}. In attempts to overcome this problem, researchers have investigated the relationships between optical properties and QD structural parameters, and the viability of controlling polarization properties has been demonstrated^{21)–31)}. However, no exact QD design and fabrication methodology has been established for practical application. In response to these circumstances, the authors have designed a novel QD structure for a polarization-insensitive QD-SOA and demonstrated its polarization-independent performance in the 1.5- μm wavelength band.

The paper is organized as follows. In Section 1, the cross-sectional aspect ratio of a QD and the strain in the QD are shown to be important factors in determining the optical polarization properties. Evidence supporting these factors is referenced from prior works based on photoluminescence (PL) characterization of bare wafers. In Section 2, the proposed columnar-QD (CQD) structure—whose aspect ratio and strain can be controlled—is described. In Section 3, the

results of an experimental study on the optical-polarization property in the columnar QDs grown under different parameters are presented. In Section 4, in regard to practical SOA fabrication, the relationship between the PL characteristics of bare wafers and the measured gain characteristics of SOA devices is investigated in terms of the polarization sensitivity. In the final section, the fabrication of optimized CQD-SOAs is described, and polarization-insensitive performance in the 1.5- μm wavelength band is demonstrated.

1. Important Factors for Determining Polarization Property

In this section, we show the evidences for that the aspect ratio and strain in QDs are important factors for controlling optical polarization¹⁹⁾⁻³¹⁾. The aspect ratio of a QD is defined as the ratio of the total height of stacked QD layers to the length of the dot base. Conventional QDs are half-oval shaped and have biaxial compressive strains, so optical transition in TE mode is predominant. It is thought that CQDs are useful for providing QDs with a high aspect ratio. The CQD is formed by growing several QD stacks, in which QDs are aligned in close contact in the vertical direction, becoming columnar in shape as a whole. The aspect ratio can be controlled by changing the number of layers of stacked QDs.

In the following, some representative results concerning InAs CQDs grown on GaAs substrates are presented. The InAs QDs were grown by molecular beam epitaxy (MBE) on a buffer layer composed of GaAs (100 nm thick), AlGaAs (50 nm), and GaAs (400 nm) formed on an n⁺-GaAs (001) substrate. The typical height of eight stacking layers was about 13 nm, and the diameter of the CQDs was about 17 nm³²⁾. Figure 1 shows the PL spectra for TE and TM polarization, which were measured from the cleaved-edge surface of CQD wafers with different stacking-layer number (SLN)²²⁾. All measurements were performed at 70 K. The

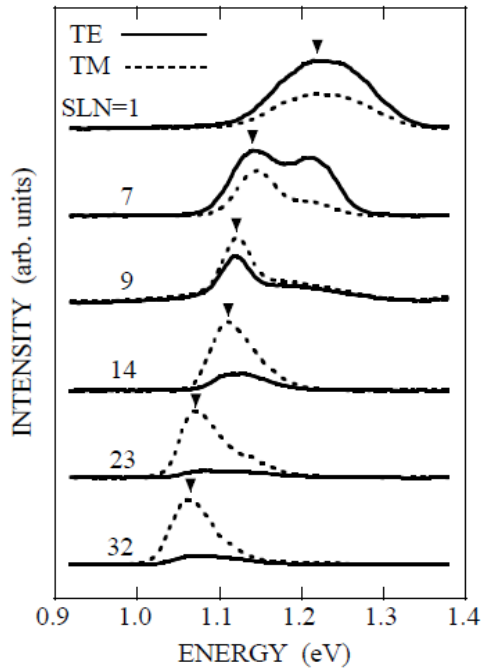


Fig. 1 TE- and TM-mode spectra of edge-emitting PL in CQDs with different SLN²²⁾.

solid and dashed lines indicate the TE- and TM-mode PL spectra, respectively. With increasing SLN, TE-mode PL intensity decreases, but TM-mode PL intensity increases. The PL peak energies, indicated by solid triangles, shift toward the lower-energy side because of the enlargement of the confinement size in the growth direction of the CQDs. As a result, the TE/TM-mode PL-intensity ratio is inverted beyond SLN of 9. The same conclusion was drawn in regard to the optical modal gain under optical pumping by using the vertical-stripe-length (VSL) technique²²⁾. When the aspect ratio is about 0.9, TM-mode transition is dominant. This is one of the lowest reported aspect ratios for obtaining TM-dominated gain.

As well as aspect ratio, relaxation of strain in QDs enhances TM-mode transition. The effect of the strain has been analyzed by theoretical calculation^{28), 29)}. The elastic-continuum theory for determining the strain distribution in the CQD and the 8-band k-p theory for modeling electronic structure were used. Figure 2 shows the hydrostatic and biaxial strain distribution in the CQDs for SLNs of 7 and 9. For SLN of 7, the biaxial strain is positive. For SLN of 9, the biaxial strain becomes negative in the fourth, fifth, and sixth layers. When the aspect ratio of the CQDs is about 0.9 (SLN=9), the strain is relaxed by the QD's shape, and the strain in the plane direction becomes tensile and larger than that in the growth direction. Under negative biaxial strain, E_{LH} is higher than E_{HH} . The transition from the conduction band to the LH band therefore predominates,

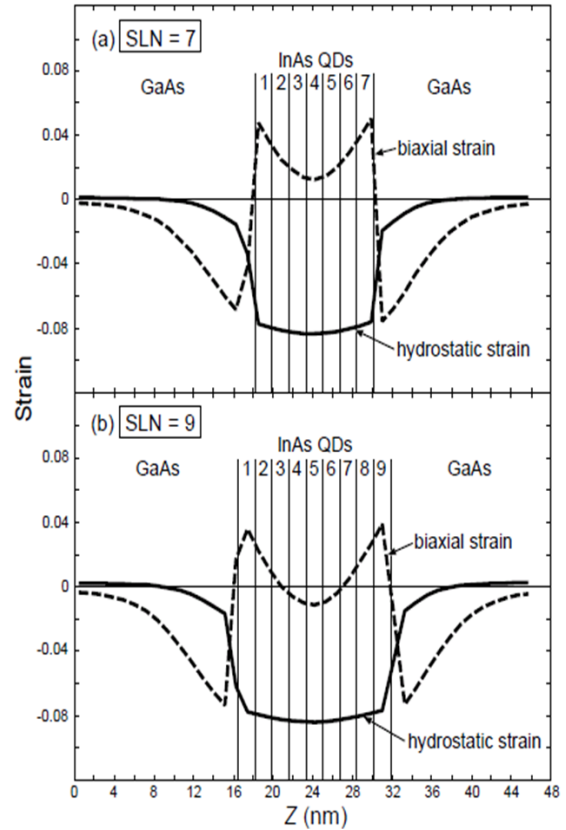


Fig. 2 Strain distribution in the columnar InAs/GaAs quantum dots for the stacking-layer number of (a) 7 and (b) 9. The hydrostatic and biaxial strain distributions on the z axis are plotted by the solid and the dashed lines, respectively. The numbers (1, 2, 3, ...) indicate each layer in the InAs quantum dots²⁹⁾.

enhancing the TM component. This result infers that the polarization-insensitive optical feature of the CQDs is due to not only the high aspect ratio but also the negative tensile biaxial strain.

We also note another phenomenon depends on QD strain, namely, thermally induced strain that occurs at different temperature between QD growth and measurement³⁰⁾. With decreasing temperature, thermal strain increases and the proportion of the TM-mode component in the ground state increases. This leads to an additional increase in the splitting energy between the HH and LH states due to thermal-strain effect. This effect should have to be taken into account when the operation temperature differs severely from the designed one.

These results indicate that the aspect ratio of a CQD and the strain in QDs are significant parameters in regard to controlling optical polarization properties of CQDs.

2. Proposed QD Structure in 1.5- μm Wavelength Band

We describe in this section our proposed QD structure which is suitable for designing polarization-insensitive QD-SOAs for 1.5- μm wavelength band optical communication systems and then the calculation of their polarization property. Figure 3 shows a schematic image of our concept. The CQD structure consists of several repetitions alternate layers of SK-mode QDs, tensile-strained side-barrier layers, and lattice-matched barriers above and below the CQD. The CQD structure focuses on two factors, namely, both increasing aspect ratio and relaxing strain in the QDs.

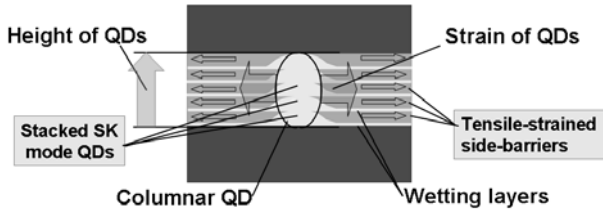


Fig. 3 Schematic image of the proposed CQD fabricated by stacking QDs.

The barrier layers above and below the CQD structure function as waveguide layers. To increase the height of the QDs, SLN is increased. In order to change the strain of the QDs from compressive to tensile, the tensile strain is applied to the side-barriers which are lattice-matched with the upper and lower barrier layers. It is not understood how the strain in QDs is related to the aspect ratio and the material surrounding the QDs. The interband optical transition energies in the 1.5- μm wavelength band of the proposed InAs/InP QD structure were calculated. The quantized energy levels of conduction and valence bands with E_{LH} and E_{HH} were calculated. In the calculation, the following assumptions were made for simplicity: box-shaped InAs QDs, base dimensions of the QDs of 15×15 nm, dot density of $7 \times 10^{10} \text{ cm}^{-2}$, strain in the side-barrier is produced by a mixed effect of the side-barrier and wetting layers (see Fig. 3), and band energy of the InGaAsP barrier corresponds to λ_g of 1.1 μm . The energy levels in the QDs embedded in the strained side-barrier were calculated. Figure 4 shows the calculated quantized energy levels of the conduction and valence bands in InAs QDs with tensile-strained side-barriers. The lattice constants of the

side-barrier surrounding the QDs are smaller by 2% (dashed lines) or 0% (solid lines) than that of the substrate. E_{LH} increases with increasing QD height for both side-barrier strains. By increasing the tensile strain of the side-barriers up to 2%, E_{LH} increases and E_{HH} decreases. E_{LH} of a 12-nm-high QD with 2% side-barrier strain is higher than the corresponding E_{HH} , so the TM-mode light is dominant over TE-mode light because the transition energy between the electrons and E_{LH} is smaller than that for E_{HH} . This result demonstrates that the columnar QD-side-barrier (CQD-SB) structure, in which CQDs with a high aspect ratio are embedded in tensile-strained side-barriers, produces a TM-mode-dominant optical transition. Moreover, it shows that polarization-insensitive gain in CQD-SB-SOAs can be produced by using QDs with high aspect ratio and by generating strain in the QDs in the range from compressive to tensile by using the strained side-barriers.

We can design the polarization-insensitive gain in CQD-SB-SOAs using both of these parameters, that is the use of a high aspect ratio of QDs and the adjustment of the strain in QDs in a range from compressive to tensile, by using the strained side-barriers.

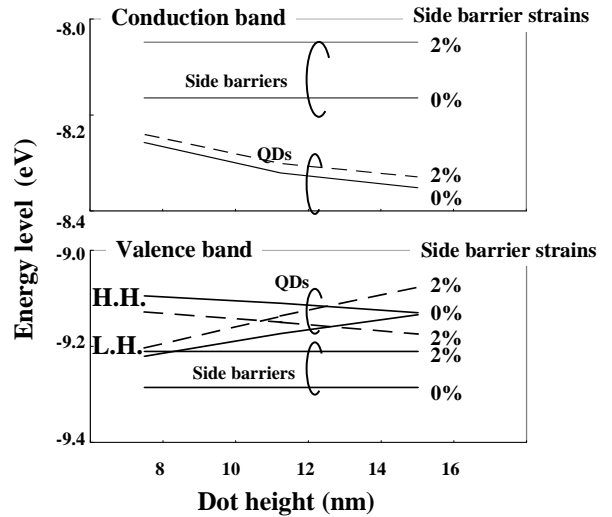


Fig. 4 Calculated energy levels of the conduction band and the valence band with 15 nm-base InAs strained side-barriers³³⁾.

3. Polarization Property of PL in CQD-SB Structure

To obtain InAs QDs (with tensile-strained InGaAsP side-barriers) with high aspect ratio, metal-organic vapor-phase epitaxy (MOVPE) was used to grow closely stacked InAs QDs on an n^+ -InP (001) substrate³⁴⁾ was used to grow closely stacked InAs QDs. The height of the CQD-SB structure was increased seven-fold to twenty five-fold to obtain a high aspect ratio. The amount of strain in the structure (hereafter, "strain amount") changed from 4% monolayer (ML) to 9.6% ML with InGaAsP side-barrier strains between 2% and 4% and thickness between 2.0 and 3.0 ML. The strain amount is defined by the product of the strain and thickness of the side-barrier. The side-barrier strains were changed by adjusting the material composition for controlling the lattice mismatch with a semiconductor substrate. The densities and the size of the QDs were determined by atomic force microscope (AFM) and cross-sectional TEM. The density of the QDs was $7.5 \times 10^{10} \text{ cm}^{-2}$. The base shape of the QDs, whose major axis in [1-10] was 22 nm and minor axis

[110] was 15 nm, was elliptical.

To investigate the polarization property, a sample with the slab-waveguide structure consisting of a 100-nm-thick InP buffer, a 100-nm-thick InGaAsP layer, a CQD-SB structure, a 50-nm-thick InGaAsP layer, and a 3- μm -thick InP cladding layer was fabricated. These structures are similar to that of actual SOA devices, except for the carrier and optical confinement structures in the lateral direction.

Polarization-dependent PL intensities were measured by exciting the [1-10] edge facets of the sample with the slab-waveguide structure. A titanium-sapphire laser with a wavelength of 810 nm and excitation power of 700 mW was focused on the edge facets, and the TE- and TM-polarized PL signals were collected from the cleaved facet by setting the polarizer along the in-plane and growth directions, respectively. The peaks around 950 nm are due to the InP bulk material showing no polarization dependence. These peaks were used to monitor polarization axis determination.

Figures 5(a) and (b) show the polarized PL spectra of CQD-SB structures with SLN of 22 and strain amounts of 7.4 and 9.3% ML³⁴⁾. We controlled the strain amount of the side-barriers surrounding the CQDs by adjusting the composition and thickness of the side-barriers. The PL spectra for the strain amount of 7.4% ML were TE-mode dominant and those for 9.3% ML were TM-mode dominant. The differences between the TE- and TM-PL intensity were 1.2 dB for the strain amount of 7.4% ML and -1.8 dB for the strain amount of 9.3% ML at a wavelength of 1.55 μm . These results

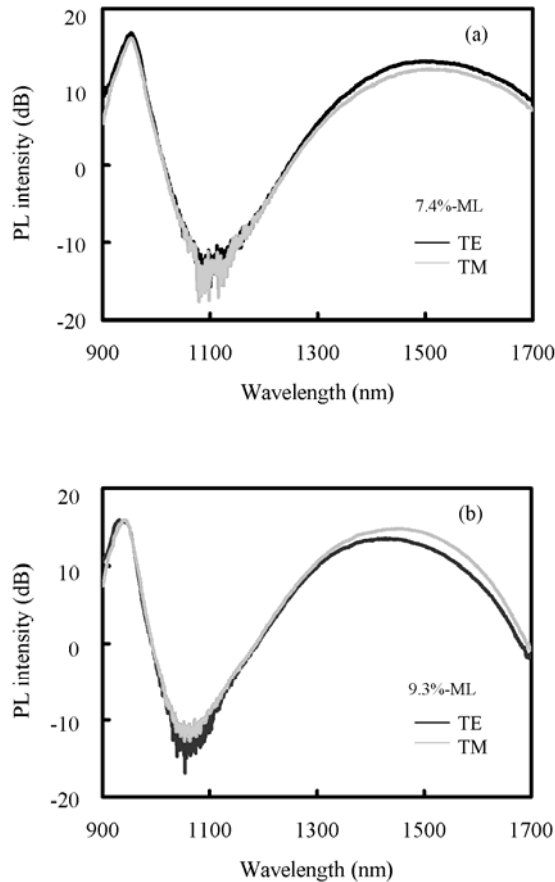


Fig. 5 The PL spectra; (a) the SLN of 22 and the strain amount of 7.4%-ML (b) the SLN of 22 and the strain amount of 9.3%-ML.

indicate that there should be an isotropic polarization point at a strain amount between 7.4 and 9.3% ML.

Figures 6(a) and (b) show the PL polarization differences as functions of SLN and the strain amount of the side-barrier at each ground-state with wavelength ranging between 1500 and 1680 nm. The TM mode increases with increasing SLN³⁴⁾. When the side-barrier strain amount increases, the TM mode light also increases. These results have revealed that the number of stacked QDs and the strain amount of the side-barriers in the CQD-SB structure can be used to effectively control polarization sensitivity of the structure. We observed that the slope of the curve become smaller at an SLN of over 13, as shown in Fig. 6 (a). The variations in the E_{LH} and E_{HH} decrease with increasing number of stacked QDs because of the size effect of the CQD-SB structures; consequently, the increments decrease. This means that there is a strain amount below which the TM-dominant transition cannot be obtained, even when SLN is large. Controlling both the strain and the aspect ratio is thus important, and the strain condition is a fundamental requirement for enabling polarization control throughout from TE to TM. In regard to practical device design and fabrication, the details of the QD growth conditions (such as growth-interruption condition) have to be readily controlled for fulfilling the wavelength and polarization requirements³⁶⁾. To optimize the CQD-SB structure for operating CQD-SB-SOAs at a wavelength of

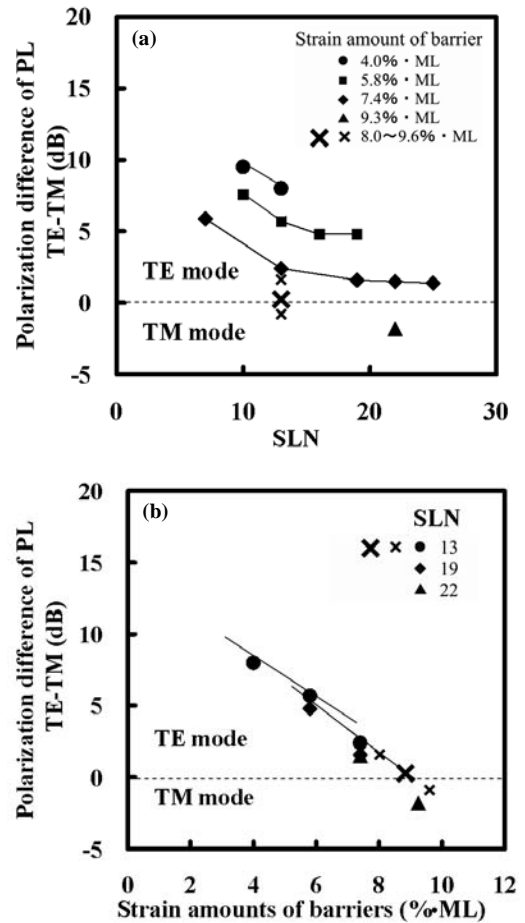


Fig. 6 (a) The polarization difference of photoluminescence PL intensity TE-TM vs. SLN (b) The polarization difference of photoluminescence PL intensity TE-TM vs. strain amount of side-barriers.

1.55 μm , we have to simultaneously adjust the wavelength in the ground state and also the polarization. The polarization-insensitive condition has been obtained in 13-fold QDs with a strain amount of 8.8% ML, as indicated by the bigger-cross plots in Figs. 6(a) and (b)³⁷⁾.

4. Application to Device Fabrication

4.1 Wafer PL vs. chip gain relationship

To apply CQD-SB structures to practical SOA devices, it is essential to grasp the relationship between the wafer PL property and SOA-device characteristics under current injection. Figure 7 shows the fabricated structure of CQD-SOAs. The InGaAsP waveguide layer was buried with conventional p-n current blocking layers. A single layer of the CQD-SB structure was placed in the center of a 320-nm-thick InGaAsP waveguide layer so that the polarization difference in the waveguide confinement factor was 10% or less. To reduce refraction at the chip facets, a tilted waveguide with an

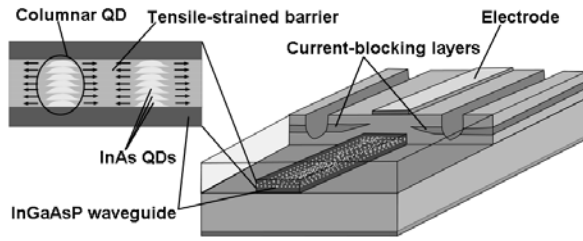


Fig. 7 Schematic image of CQD-SOA.

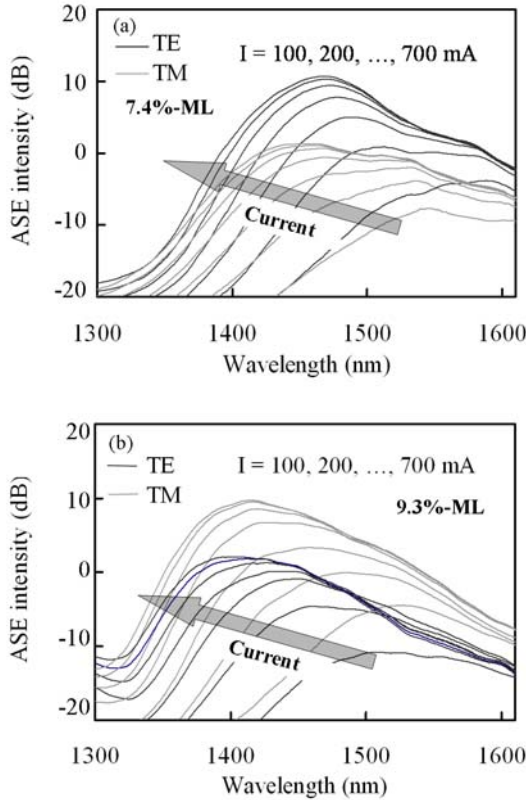


Fig. 8 Polarization ASE spectra between 1300 and 1610 nm at the drive current ranging from 100 to 700 mA; (a) the SLN of 22 and the strain amount of 7.4%-ML (b) the SLN of 22 and the strain amount of 9.3%-ML.

8-degree off-angle and an anti-reflection coating was used²⁾.

To confirm the polarization property under current injection, the polarized amplified spontaneous emission (ASE) and gain spectra of SOAs fabricated with the two types of CQD-SB structures described above were measured. The device length was 2 mm. The chip was characterized for CW (continuous wave) signals by varying the chip current from 100 to 700 mA. Figures 8(a) and (b) show the spectra of TE- and TM-mode ASEs for SLN of 22 and strain amounts of 7.4 and 9.3% ML, respectively. The TE- and TM-ASEs were measured by collimating the emission from the cleaved facet and collecting the TE- and TM-polarized signals with a polarizer. The ASE spectra for 9.3% ML were TM-mode dominant. The intensity of the TE- and TM-mode ASE at a wavelength of 1.55 μm saturates beyond 400 mA. The differences between the TE- and TM-mode ASEs were 5.3 dB for strain amount of 7.4% ML and -8.2 dB for strain amount of 9.3% ML at a wavelength of 1.55 μm .

Figures 9(a) and (b) show the spectra for TE and TM gain. A polarization scanning technique was used to measure the polarization characteristics (Agilent 11896A). The gain spectra of CQD-SB structure with the strain amount of 7.4% ML show a greater TE-mode intensity than that of the TM mode. The gain spectra of CQD-SB structure with the strain amount of 9.3% ML show greater TM-mode intensity than that of the TE mode. The polarization dependence of gain (PDG) ($G_{\text{TE}} - G_{\text{TM}}$) of SOAs was 5.5 dB for the strain amount of 7.4% ML and -7.0 dB for the strain amount of 9.3% ML. The PDG spectra exhibit a tendency similar to those of the ASE, although two spectra-measurement systems, namely, a free-space-based system and an optical-fiber-based system,

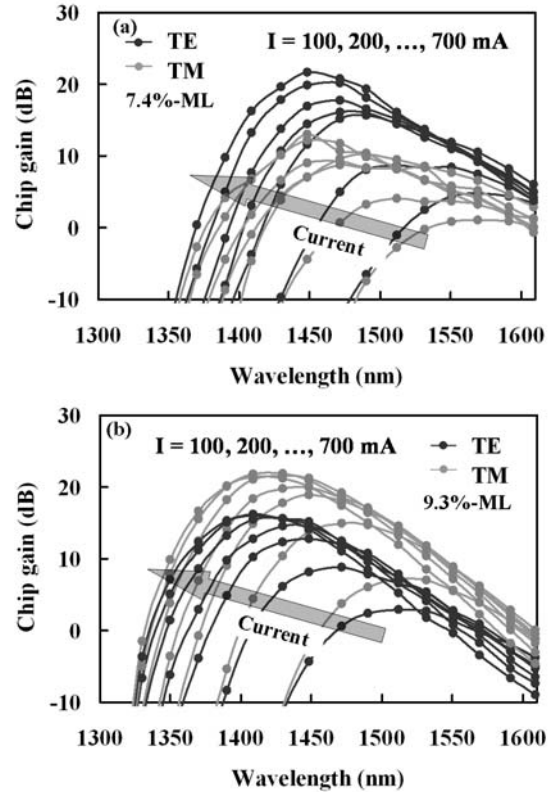


Fig. 9 Chip gain spectra between 1300 and 1610 nm at the drive current ranging from 100 to 700 mA; (a) the SLN of 22 and the strain amount of 7.4%-ML (b) the SLN of 22 and the strain amount of 9.3%-ML.

were used.

To achieve polarization insensitivity in the QD-SOAs, the optical properties of the CQD-SB structures must be controlled precisely. The relationship between the polarization dependence of the PL intensity in CQD-SB wafers and the optical polarization characteristics of resultant devices was therefore investigated in detail. For this purpose, various kinds of CQD-SB structures were fabricated and evaluated.

Figure 10 shows PDG evaluated at average gain $((G_{TE}+G_{TM})/2)$ of 10 dB versus polarization dependence of PL intensity ($I_{TE}-I_{TM}$) at a wavelength of 1.55 μm . We chose a drive current of 600 mA for which the gain saturates. The error in PDG was less than ± 0.1 dB, and the error in polarization-dependence was less than ± 0.015 dB. PDG is almost directly proportional to the polarization dependence of PL intensity. Polarization-independent operation of the SOA at a wavelength of 1.55 μm is obtained at the point of PL-polarization dependence equal to 0.3 dB. To obtain polarization dependence of gain of less than ± 0.5 dB at a chip gain of 10 dB, the PL-polarization dependence must be 0.3 ± 0.1 dB.

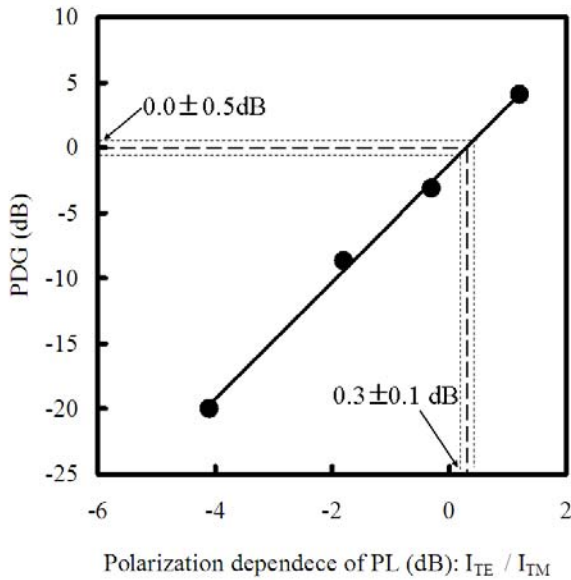


Fig. 10 Polarization dependence of chip gain vs. polarization dependence of wafer PL.

4.2 SOA characteristics

To demonstrate the polarization-independent operation, SOAs with optimized CQD-SB structures were fabricated. Referring to the correlation as shown in Fig. 10, the CQD-SB structural parameters in the bigger-cross plots in Figs. 6 (a) and (b)³⁷⁾ were investigated. These parameters correspond to a polarization difference in PL intensity of 0.15 dB at a wavelength of 1.55 μm . The structure was optimized at the SLN of 13 with a strain amount of 8.8% ML³⁶⁾. Other parameters used for the device structures are similar to the ones described in Fig. 7. The SOA chip was characterized for CW signals at 25°C. The device length was 6 mm. Figure 11 shows the chip gain and PDG at a wavelength of 1.55 μm as functions of drive current. The gain appears at the drive current of 200 mA and saturates at 10.0 dB beyond 600 mA. The PDGs are less than ± 0.9 dB in the drive current range from 100 to 1200 mA. It would be worthwhile mentioning

that this device achieved error-free operation at a bit rate of 40 Gbit/s, the detail of which will be published elsewhere. It is thus concluded that an SOA with a very low PDG at the wavelength of 1.55 μm can be produced by optimizing the CQD-SB structure.

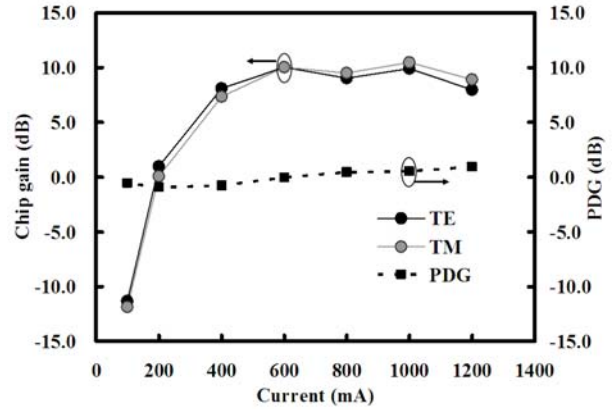


Fig. 11 The chip-gain characteristics as a function of drive current at the wavelength of 1.55 μm .

Summary

A technique for fabricating polarization-insensitive QD-SOAs was developed, and the polarization independent performance of the QD-SOAs was demonstrated. It was found that both the aspect ratio and strain of QDs are important and useful parameters for controlling polarization sensitivity. To control these two parameters, a novel CQD-SB structure that consists of columnar QDs embedded in tensile-strained side-barriers was fabricated. It was found that this structure enables polarization-insensitive operation in the 1.5- μm wavelength band. The relationship between the CQD-SB structures and the optical polarization characteristics of resultant devices was investigated. Polarization-independent photoluminescence (PL) was achieved in CQDs that have a 13-fold by using tensile-strained side-barriers with a strain amount of 8.8% ML. The fabricated CQD-SB-SOAs have a gain of 10.0 dB with PDG of ± 0.9 dB at a wavelength of 1.55 μm . These results indicate that CQD-SB-SOAs can be used as a basic polarization-insensitive SOA device for future very-high-speed optical communication systems.

Reference:

- 1) M. Sugawara, H. Ebe, N. Hatori, M. Ishida, Y. Arakawa, T. Akiyama, K. Otsubo, and Y. Nakata, "Theory of optical signal amplification and processing by quantum-dot semiconductor optical amplifiers," *Phys. Rev.*, vol. B 69, 235332(1-39) (2004)
- 2) T. Akiyama, M. Ekawa, M. Sugawara, K. Kawaguchi, H. Sudo, A. Kuramata, H. Ebe, and Y. Arakawa, "An ultrawide-band semiconductor optical amplifier having an extremely high penalty-free output power of 23 dBm achieved with quantum dots," *IEEE Photonics. Technol. Lett.*, vol. 17, 1614-1616 (2005)
- 3) A. Bilenca, R. Alizon, V. Mikhelashvili, D. Dahan, G. Eisenstein, R. Schwertberger, D. Gold, J. P. Reithmaier, and A. Forchel, "Broad-Band wavelength conversion based on cross-gain modulation and four-wave mixing in InAs-InP quantum-dash semiconductor optical amplifier

- at 1.55 μm ,” *IEEE Photonics Technol. Lett.*, vol. 15, 563-565 (2003)
- 4) A. Bilenca, R. Alizon, Mikhelashvili, G. Eisenstein, R. Schwerberger, D. Gold, J.P. Reithmaier and A. Forchel, “InAs/InP 1550 nm quantum dash semiconductor optical amplifiers,” *Electron. Lett.*, Vol. 38, 1350-1351 (2002)
- 5) T. Akiyama, H. Kuwatsuka, S. Simoyama, Y. Nakata, K. Mukai, S. Sugawara, O. Wada, and H. Ishikawa, “Nonlinear gain dynamics in quantum-dot optical amplifier and its application to optical communication devices,” *IEEE J. Quantum Electron.*, vol. 37, 1059-1065 (2001)
- 6) T. Akiyama, N. Hatori, Y. Nakata, H. Ebe, and M. Sugawara, “Pattern-effect-free semiconductor optical amplifier achieved using quantum dots,” *Electron. Lett.*, Vol. 38, 1139-1140 (2002)
- 7) M. Sugawara, N. Hatori, T. Akiyama, Y. Nakata, and H. Ishikawa, “Quantum-dot semiconductor optical amplifiers for high bit-rate signal processing over 40Gbit/s,” *Jpn. J. Appl. Phys.*, Vol. 40, L488-491 (2001)
- 8) S. Schneider, P. Borri, W. Langbein, U. Woggon, R. L. Sellin and D. Bimberg, “Excited-state gain dynamics in InGaAs Quantum-dot Amplifiers,” *IEEE Photonics Technol. Lett.*, vol.17, 2014-2016 (2005)
- 9) S. Dommers, V. V. Temnov, U. Woggon, J. Gomis, J. Martinez-Pastor, M. Laemmlin, and D. Bimberg, “Complete ground state gain recovery after ultrashort double pulses in quantum dot based semiconductor optical amplifier,” *Appl. Phys. Lett.*, Vol. 90, 033508(1-3) (2007)
- 10) I. O’Driscoll, T. Piwonski, C.-F. Schleussner, J. Houlihan, G. Huyet, and R. J. Manning, “Electron and hole dynamics of InAs/GaAs quantum dot semiconductor optical amplifiers,” *Appl. Phys. Lett.*, Vol. 91 071111(1-3) (2007)
- 11) T. Vallaitis, C. Koos, R. Bonk, W. Freude, M. Laemmlin, C. Meuer, D. Bimberg, J. Leuthold, “Slow and fast dynamics of gain and phase in a quantum dot semiconductor optical amplifier,” *Opt. Express*, Vol. 16, 170-178 (2008)
- 12) V. Cesari, P. Borri, M. Rossetti, A. Fiore, and W. Langbein, “Refractive Index Dynamics and linewidth enhancement factor in *p*-Doped InAs–GaAs Quantum-Dot Amplifiers,” *IEEE J. Quantum Electron.*, Vol. 45, 579-585 (2009)
- 13) C. Meuer, J. Kim, M. Laemmlin, S. Liebich, D. Bimberg, A. Capua, G. Eisenstein, R. Bonk, T. Vallaitis, J. Leuthold, A. R. Kovsh, and I. L. Krestnikov, “40 GHz small-signal cross-gain modulation in 1.3 μm quantum dot semiconductor optical amplifier,” *Appl. Phys. Lett.*, Vol. 93, 051110 (1-3) (2008)
- 14) G. Grobkopf, R. Ludwig, R. G. Waarts, H. G. Weber, “Optical amplifier configurations with low polarization sensitivity,” *Electron. Lett.*, Vol.23, 1387-1388 (1987)
- 15) N. A. Olsson, “Polarization-independent configuration optical amplifier,” *Electron. Lett.*, vol. 24, 1075-1076 (1988)
- 16) I. Cha, M. Kitamura, H. Honmou, I. Mito, “1.5- μm band travelling-wave semiconductor optical amplifiers with window facet structure,” *Electron. Lett.*, vol. 25, 1241-1242 (1989)
- 17) K. Magari, M. Okamoto, Y. Suzuki, K. Sato, Y. Noguchi, and O. Mikami, “Polarization-insensitive optical amplifier with tensile-strained-barrier MQW structure,” *IEEE J. Quantum Electron.*, vol. 30, 695-701 (1994)
- 18) K. Morito, M. Ekawa, T. Watanabe, and Y. Kotaki, “High-output-power polarization-insensitive semiconductor optical amplifier,” *J. Lightwave Technol.*, vol. 21, 176-181 (2003)
- 19) O. Stier, M. Grundmann, and D. Bimberg. “Electronic and optical properties of strained quantum dots modeled by 8-band k-p theory,” *Phys. Rev.*, vol. B 59, 5688-5701 (1999)
- 20) W. Sheng, and J-P Leburton “Interband transition distributions in the optical spectra of InAs/GaAs self-assembled quantum dots,” *Appl. Phys. Lett.* Vol. 80, 2755-2757 (2002)
- 21) P. Yu, W. Langbein, K. Leosson, and J. M. Hvam, “Optical anisotropy in vertically coupled quantum dots,” *Phys. Rev.*, vol. B 59, 16680-16685 (1999)
- 22) T. Kita, O. Wada, H. Ebe, Y. Nakata, and M. Sugawara, “Polarization-independence photoluminescence from columnar InAs/GaAs self-assembled quantum dots,” *Jpn. J. Appl. Phys.*, vol. 41, L1143-L1145 (2002)
- 23) T. Kita, N. Tamura, O. Wada, M. Sugawara, Y. Nakata, H. Ebe, and Y. Arakawa, “Artificial control of optical gain polarization by stacking quantum dot layers,” *Appl. Phys. Lett.*, vol. 88, 211106(1-3) (2006)
- 24) P. Ridha, L. Li, A. Fiore, G. Patriarche, M. Mexis, and P. M. Smowton, “Polarization dependence study of electroluminescence and absorption from InAs/GaAs columnar quantum dots” *Appl. Phys. Lett.*, vol. 91, 191123(1-3) (2007)
- 25) S. Anantathanasarn, R. Nötzel, P. J. van Veldhoven, F. W. M. van Otten, T. J. Eijkemans, and J. H. Wolter, “Stacking and polarization control of wavelength-tunable (1.55 μm region) InAs/InGaAsP/InP (100) quantum dots,” *Appl. Phys. Lett.*, vol. 88, 063105(1-3) (2006)
- 26) S. Anantathanasarn, P. J. van Veldhoven, T. J. Eijkemans, T. de Vries, E. Smalbrugge, E. J. Geluk, E. A. J. Bente, Y. S. Oei, M. K. Smit, and R. N. Nötzel, “Polarization control of gain of stacked InAs/InP (100) quantum dots at 1.55 μm : Interplay between ground and excited state transition,” *Appl. Phys. Lett.*, vol. 92, 123113(1-3), (2008)
- 27) K. Kawaguchi, M. Ekawa, N. Yasuoka, T. Akiyama, H. Ebe, M. Sugawara, and Y. Arakawa, “1.3-1.6 μm broadband polarization-independent luminescence by columnar InAs quantum dots on InP(001),” *Phys. Stat. Sol.(c)*, vol. 3, 3646-3651 (2006)
- 28) T. Saito, T. Nakaoka, T. Kakitsuka, Y. Yoshikuni, Y. Arakawa, “Strain distribution and electronic states in stacked InAs/GaAs quantum dots with dot spacing 0-6 nm,” *Physica*, vol. E 26, 217-221 (2005)
- 29) T. Saito, H. Ebe, Y. Arakawa, T. Kakitsuka, M. Sugawara, “Optical polarization in columnar InAs/GaAs quantum dots: 8-band k-p calculations,” *Phys. Rev.*, vol. B 77, 195318(1-11) (2008)
- 30) P. Jayavel, H. Tanaka, T. Kita, O. Wada, H. Ebe, M. Sugawara, Y. Arakawa, Y. Nakata, and T. Akiyama, “Optical polarization properties of InAs/GaAs quantum dots semiconductor optical amplifier,” *Jpn. J. Appl. Phys.*, vol. 44, 2528-2530 (2005)
- 31) P. Jayavel, H. Tanaka, Kita, O. Wada, H. Ebe, M. Sugawara, J. Tatebayashi, Y. Arakawa, Y. Nakata, and T. Akiyama, “Control of optical polarization anisotropy in edge emitting luminescence of InAs/GaAs self-assembled quantum dots,” *Appl. Phys. Lett.*, vol. 44, 1820-1822 (2004)
- 32) Y. Nakata, Y. Sugiyama, K. Mukai, T. Futatsugi, H. Shoji, M. Sugawara, H. Ishikawa, and N. Yokoyama, “columnar-shaped InAs/GaAs self-assembled quantum

- dots grown by molecular beam epitaxy,” *Inst. Phys. Conf.*, No.162: Chapter 9 427-432 (1998)
- 33) H. Ebe, A. Uetake, T. Akiyama, K. Kawaguchi, M. Ekawa, A. Kuramata, Y. Nakata, M. Sugawara, and Y. Arakawa, “Internal strain of self-assembled $\text{In}_x\text{Ga}_{1-x}\text{As}$ quantum dots calculated to realize transverse-magnetic-mode-sensitive interband optical transition at wavelength of 1.5 μm bands,” *Jpn. J. Appl. Phys.*, vol. 44, 6312-6316 (2005)
 - 34) K. Kawaguchi, N. Yasuoka, M. Ekawa, H. Ebe, T. Akiyama, M. Sugawara, and Y. Arakawa, “Controlling polarization of 1.55- μm columnar InAs quantum dots with highly tensile-strained InGaAsP barriers on InP(001) ,” *Jpn. J. Appl. Phys.*, vol. 45, L1244-L1246 (2006)
 - 35) N. Yasuoka, K. Kawaguchi, H. Ebe, T. Akiyama, M. Ekawa, S. Tanaka, K. Morito, M. Sugawara, and Y. Arakawa, “Demonstration of transverse-magnetic dominant gain in quantum dot semiconductor optical amplifiers,” *Appl. Phys. Lett.*, vol. 92, 101108(1-3) (2008)
 - 36) K. Kawaguchi, N. Yasuoka, M. Ekawa, H. Ebe, T. Akiyama, M. Sugawara, and Y. Arakawa, “Optical properties of columnar InAs quantum dots on InP for semiconductor optical amplifier,” *Appl. Phys. Lett.*, vol. 93, 121908(1-3) (2008)
 - 37) N. Yasuoka, K. Kawaguchi, H. Ebe, T. Akiyama, M. Ekawa, K. Morito, M. Sugawara, and Y. Arakawa, “Quantum-dot semiconductor optical amplifiers with polarization-independent gains in 1.5- μm wavelength bands, ” *IEEE Photonics. Technol. Lett.*, vol. 20, 1908-1910 (2008)